END
DATE
FILMED
8-82
DTIC

Cont

A
329

AD A116292

HYDRODYNAMIC TEST FACILITIES AT ARL/PSU

R. E. Henderson and B. R. Parkin

The Pennsylvania State University
APPLIED RESEARCH LABORATORY
Post Office Box 30
State College, PA 16801

NAVY DEPARTMENT

NAVAL SEA SYSTEMS COMMAND

DTIC
SELECTED
JUN 30 1982

D

82 06 30 044

DTIC FILE COPY

REPORT DOCUMENTATION PAGE		READ INSTRUCTIONS BEFORE COMPLETING FORM
1. REPORT NUMBER TM 82-66	2. GOVT ACCESSION NO. AD-A116 292	3. RECIPIENT'S CATALOG NUMBER
4. TITLE (and Subtitle) HYDRODYNAMIC TEST FACILITIES AT ARL/PSU		5. TYPE OF REPORT & PERIOD COVERED Technical Memorandum
		6. PERFORMING ORG. REPORT NUMBER
7. AUTHOR(s) R. E. Henderson and B. R. Parkin		8. CONTRACT OR GRANT NUMBER(s) N00024-79-C-6043
9. PERFORMING ORGANIZATION NAME AND ADDRESS Applied Research Laboratory Post Office Box 30 State College, PA 16801		10. PROGRAM ELEMENT, PROJECT, TASK AREA & WORK UNIT NUMBERS
11. CONTROLLING OFFICE NAME AND ADDRESS Naval Sea Systems Command Department of the Navy Washington, DC 20362		12. REPORT DATE 12 February 1982
		13. NUMBER OF PAGES 40
14. MONITORING AGENCY NAME & ADDRESS(if different from Controlling Office)		15. SECURITY CLASS. (of this report) UNCLASSIFIED
		15a. DECLASSIFICATION/DOWNGRADING SCHEDULE

16. DISTRIBUTION STATEMENT (of this Report)

Approved for public release. Distribution unlimited
Per NAVSEA -   March 2, 1982.

17. DISTRIBUTION STATEMENT (of the abstract entered in Block 20, if different from Report)

18. SUPPLEMENTARY NOTES

19. KEY WORDS (Continue on reverse side if necessary and identify by block number)

hydrodynamics, test, facilities, water tunnels

20. ABSTRACT (Continue on reverse side if necessary and identify by block number)

A discussion is presented of the major advances in hydrodynamic testing which have been demonstrated in the Fluids Engineering Department during the past 15 years.

DD $_{1\ JAN\ 73}^{FORM}$ 1473   EDITION OF 1 NOV 65 IS OBSOLETE

Subject: <u>Hydrodynamic Test Facilities at ARL/PSU</u>

References: See page 15.

Abstract: A discussion is presented of the major advances in hydrody-
            namic testing which have been demonstrated in the Fluids
            Engineering Department during the past 15 years.

12 February 1982
                                         REH:BRP:cag

Table of Contents

1.0 INTRODUCTION

The design and operational characteristics of the 1.22 m diameter,
high speed water tunnel (the Garfield Thomas Water Tunnel) operated by
the Fluids Engineering Department of the Applied Research Laboratory,
the Pennsylvania State University (ARL/PSU) have been documented in a
number of reports and papers written during its first 18 years of
operation [1-3]. Since the last of these papers was written in 1967,
the capabilities of the Garfield Thomas Water Tunnel (GTWT) to address
hydrodynamic problems have been significantly extended. These new
capabilities include: (1) the measurement of cavitation noise and
noise in the absence of cavitation; (2) the measurement of the dynamic
forces generated on model propulsors operating on a model vehicle;
(3) the reduction of the turbulence level in its test section to
0.1% with an integral scale of 1.25 cm, by the addition of honey-
comb in the settling section; and (4) the development of electro-
optical measuring techniques. In addition to these new capabilities,
efforts have continued in the area of tunnel/model interference and
its influence on model drag. By the use of tunnel wall flow
correcting liners, it is possible to predict accurately the
propulsion characteristics of large powered models.

The purpose of this paper is to discuss these developments in the
hydrodynamic experimental capabilities of the GTWT during the past
15 years. Also to be discussed are a number of complimentary test
facilities, both water and air tunnels, which contribute to the
solution of hydrodynamic problems. These discussions will be accom-
panied by examples of test results which demonstrate the successful
employment of these test facilities.

2.0 DESCRIPTION OF FACILITIES

In the following discussion of the hydrodynamic experimental
capabilities at ARL/PSU, results obtained from experiments conducted
in five of its major test facilities will be presented. These
facilities include:

(1) the Garfield Thomas Water Tunnel (GTWT) with its 1.22 m x 4.27 m
     cylindrical test section and a maximum test section velocity of
     18.29 m/s;

(2) the "small" water tunnel which has both a 0.305 m x 0.762 m
     cylindrical and a 0.508 m x 0.114 m x 0.762 m rectangular test
     section with a maximum test section velocity of 24.38 m/s;

(3) the 0.152 m diameter water tunnel with a maximum velocity of
     27.4 m/s which can be used as a closed circuit pump loop;

(4) the ultra-high speed water tunnel with a 38.1 mm diameter test
     section and a maximum velocity of 83.8 m/s; and

(5) the axial flow research fan which is an open-circuit subsonic
     air tunnel used to study the steady and dynamic flow through
     propulsor blade rows.

A complete description of the operating characteristics of each of
these facilities, together with a circuit schematic, can be found in
Appendix A.

3.0 VEHICLE POWERING TESTS

The standard facility used to determine the powering or propul-
sion characteristics of a marine vehicle is the towing tank, and is
essential for the determination of wave drag. They are also useful
for cases in which free-surface effects are not important, such as
completely submerged vehicles. However, towing tank tests to determine
the propulsion characteristics of a completely submerged vehicle will
usually have a limiting test velocity of the order of 5-8 m/s due to
the effects of surface waves and water-piercing strut interference
drag. The resulting Reynolds number is then often too low to allow
accurate scaling of the powering data to the prototype vehicle.

Surface interference effects can be eliminated for completely
submerged vehicles by conducting the powering tests in a water tunnel.
In a large water tunnel the tests can usually be conducted at higher
test velocities, 10-12.2 m/s in the GTWT, and hence at higher Reynolds
numbers than in a towing tank with the same model. The attainment
of higher Reynolds numbers minimizes the possible errors in scaling
the powering data. At the same time, the water tunnel allows propulsor
cavitation characteristics to be determined with the propulsor operated
in the vehicle boundary layer. While these points are obvious advan-
tages in the testing of completely submerged vehicles, the additional
factors of tunnel wall interference and horizontal buoyancy must be
considered.

In the late 1950's a study was conducted at ARL/PSU on the use of
tunnel wall flow correcting liners to minimize these drag inter-
ference effects [4], [5]. The usefulness of this technique depends
upon the accurate calculation of the flow field over the model when
operated both with and without the tunnel walls present. The tunnel
walls are then altered for each model by inserting a tunnel wall liner
which is designed to give, except for fluid-frictional effects, the
same flow over the model as it is predicted to experience without the
tunnel walls present, i.e., a "free-field" condition, Figure 1.

The use of tunnel wall liners has proven to be a very successful
means to provide the same boundary layer velocity profile at the
aft-end of a model as measured in a towing tank or in a very large
wind tunnel where model/wall interference is negligible. In the case
of models whose total length is greater than the test section length,
4 m, a section of the model's parallel mid-section must be removed.

This removed section is simulated by the addition of a screen, or screens, on the remaining vehicle surface. The length of screen is selected so as to add the same frictional resistance as the removed parallel midsection. This provides the same boundary layer velocity profile as with the complete model. Figure 2 shows the agreement of the circumferential mean velocity profile measured on a shortened 0.61 m maximum diameter model in the 1.22 m diameter test section with data measured with a total length model in a towing tank.

Experience has shown that while the liners provide a correct velocity distribution, they cannot be designed, manufactured and installed with sufficient accuracy to eliminate completely the effects of horizontal buoyancy on vehicle drag [5]. During the past 10 years a study of this problem has shown that it is possible to correct empirically for these inaccuracies. Experience and the theory of interference for an axially symmetric body in a circular test section [1] indicate that if the ratio of the model diameter (d) to the test section diameter (D) is less than 1/9, the interference drag will be within the accuracy of the drag measurements. It is therefore possible to measure the drag on a scaled model whose $d < D/9$, calculate the residual or pressure drag coefficient of the model by subtracting the calculated friction drag coefficient from the measured total drag, assume that the residual drag coefficient does not change with Reynolds number, and calculate the total drag coefficient of a model whose $d > D/9$ as a function of Reynolds number. Since this calculation does not include the effects of tunnel wall interference, it represents a baseline or reference for tests with the large model. These same reference data can also be obtained from tests of the large model in a towing tank.

Once the variation of model drag coefficient with Reynolds number is known, these data can be used to "calibrate" the tunnel/model installation and determine the wall interference and horizontal buoyancy associated with the large model, Figure 3. This represents a correction which must be applied to the net axial force, thrust-drag, on a model with an operating propeller. The use of a tunnel wall liner then assures that the propeller operates in the correct boundary layer profile and it minimizes the magnitude of the wall interference correction. Recent tests using liners constructed of fiberglass segments and a model of $d = 0.53D$, showed this correction to be approximately 8 percent of the total model drag.

Figure 4 shows a example of the application of this procedure to the prediction of the powering performance of a particular vehicle. This figure compares the velocity of a completely submerged vehicle and its propeller torque as predicted from water tunnel tests with values measured during free-running field trials.

4.0 CAVITATION TESTS

At the ARL/PSU, cavitation tests are conducted in the 1.22 m,
0.305 m, 0.147 m, and 3.81 cm water tunnels. In the 1.22 m GTWT most
of the cavitation studies are concerned with cavitation inception,
cavitation noise and cavitation scaling experiments on large scale
bodies, hydrofoils and propellers. The 0.305 m tunnel is used to
conduct fundamental studies of cavitation scaling, vortex cavitation,
cavitation noise, and both ventilated and supercavitating flows with
small scale stationary bodies and hydrofoils. The influence of
polymers on cavitation inception and scaling have been studied in
the 0.147 m tunnel, together with cavity flows on hydrofoils. The
small, ultra-high speed 3.81 cm tunnel was originally built by
NASA to study thermodynamic effects on cavitation in a liquid operating
near its critical point. In addition, the NASA tunnel has been used to
study the effect of velocity on cavitation damage since it can attain a
maximum velocity of 83.8 m/s.

Generally, the kinds of measurements needed for cavitation
research are the same as those required for the study of non-cavitating
flows. This is so because it is first necessary to understand the
non-cavitating flow and to then relate its characteristics to the
conditions under which cavitation occurs. However, certain experi-
mental techniques have become particularly useful in cavitation
research and these techniques will be emphasized here.

4.1 Nuclei Measurements

An important research topic these days is the determination of
the way cavitation nuclei influence the occurrence of cavitation.
Although present knowledge on this subject is incomplete, a number
of investigators around the world are studying various aspects of
this problem using various methods of measurement. At ARL/PSU both
light-scattering and holographic techniques have been used with the
emphasis on the measurement of free-stream nuclei size distributions.
For example, it was found in a joint research program with the
California Institute of Technology (CIT) [6] that light scattering
and holographic measurements produced significantly different nuclei
size distributions when measurements were made by both methods in the
same facility. Such dual measurements were made at CIT in their High
Speed and Low Turbulence tunnels [7], [8], and supplementary light-
scattering measurements were made in the ARL/PSU 0.305 m tunnel.
In these experiments the light-scattering unit was of a type similar
to that proposed by Keller [9]. The single detector/counter used is
illustrated in Figure 5 and the calibration curves shown in Figure 6
compare the results obtained at CIT and ARL/PSU. Comparative nuclei
distributions measured by the light scattering and holographic
techniques in the CIT High Speed Water Tunnel are shown in Figure 7.
A schematic of the holographic apparatus is shown in Figure 8. It

was concluded from these experiments that the light scattering tech-
nique was not able to discriminate between solid particles and air
bubbles in the flow.

As a result of these findings, recent studies at ARL/PSU have
concentrated on the development of a dual-detector technique which,
with the use of Mie-scattering theory, can give information about the
shape of the particle. This permits the light scattering technique
to discriminate between microbubbles and particulates, Figure 9.
The results to date indicate that this modified Keller system offers
the potential of screening particulates from the microbubble counts
[10]. The main task remaining before this approach can be called
successful is to conduct a detail error analysis in order to resolve
the system inaccuracy introduced by the data reduction algorithm.
Because the light scattering technique offers the chance of getting
nearly real-time nuclei distribution data while a cavitation test
is in progress, this improvement of the Keller system is worth
pursuing.

Assuming that valid nuclei size distributions can be obtained
while a cavitation experiment is underway, the question of how such
distributions influence the development of cavitation on a body must
be studied. Such a study can be conducted if the cavitation events
can be related to such flow features as the boundary layer thickness
or whether or not the flow is separated. Schlieren flow visualization
is an effective way to show the relationship of cavitation inception
and its type to the state of the boundary layer [11]. Measurements of
this type have been performed in the ARL/PSU 0.305 m tunnel using
light scattering and schlieren systems simultaneously as illustrated
in Figure 10 [12].

Of course holographic photography can be used for flow visualiza-
tion with excellent results in both cavitating and non-cavitating
flows.

4.2 Cavitation Damage

In the introductory remarks of this section it was noted that
one use of the NASA tunnel and its very high velocity, has been to
study the process of cavitation damage [13]. Recent studies at
ARL/PSU have confirmed the sixth-power of the free-stream velocity
scaling relation reported by previous investigators. In these
studies it was possible to obtain nearly a four-fold increase in
velocity, from about 15 m/s to 60 m/s. A fact not previously
reported is that the pitting rate in the incubation zone is sensitive
to, and inversely proportional to, the dissolved air content.
Therefore it was possible to correct all of the data to a standard
air content of 8.9 ppm so that data for all investigations over a
10,000 to 1 range in damage rates could be brought into remarkable
agreement, Figure 11. It is important to stress that this investi-

gation involved the study of pitting on a body with the occurrence of weight loss. With this restriction it was found that damage in the form of individual pits had a one-to-one correspondence with the cavitation bubble collapse energy, and the change in this energy with free-stream velocity could be inferred.

5.0 ACOUSTIC TESTS

The GTWT was designed to provide the capability to conduct research on torpedo propellers operated in a specified vehicle/ control fin wake [1]. With the wake flow produced by the installation of the actual vehicle or a scaled model, the measurement of the forces on the vehicle and its propeller and the occurrence of cavitation on the propeller were the primary performance characteristics studied. While the inception of cavitation was detected acoustically, as well as visually, the GTWT was not used to conduct detailed acoustic tests during its first 20 years of operation. Fortunately, the design of the GTWT was directed towards quiet and vibration free operation. The success in achieving these goals has permitted the development of a capability to conduct tests of both cavitating and non-cavitating propeller noise.

5.1 Cavitation Noise

The GTWT was designed so that one side of its test section could be fitted with an acoustic tank in which a traversing reflector hydrophone could be mounted, Figure 12. With the hydrophone focused on the centerline of the test section, it measures the noise radiated from a model located opposite the 27 cm x 60 cm plexiglass windows.

The receiver is a Celesco LC-10 hydrophone located at the focus of the ellipsoidal reflector. This hydrophone is calibrated by placing an omni-directional sound projector with a known response in the test section and driving it over a frequency range of 1-120 kHz. The calibration is conducted with the sound projector located on the test section centerline and at a constant distance off-centerline in each of four or more circumferential positions, Figure 13. This latter approach permits an average sensitivity to be determined diminishes the influence of spurious acoustic modes that are observed when the projector is on the centerline. It is also more representative of the noise radiated by a propeller since cavitation will normally appear first near the tip of the blades.

The influence of the test section on the directivity of the reflector hydrophone is shown by Figure 14. In this figure the directivity measured at 20 kHz in the test section is compared with the same measurement conducted in the free field [14]. It is obvious that this arrangement is acceptable if the hydrophone is positioned in the center of the window, but is restricted by the metal webs between the windows. To overcome this restriction an

acoustically transparent hatch cover has been procurred for the GTWT.
This special hatch replaces the original metal access cover to the
test section with a large (0.4 m x 3.0 m) continuous plexiglass
window. A tank is located over this large window which is filled
with water and allows the installation of additional hydrophones.
This permits an unobstructed acoustical scanning of the model in
the test section. This new hatch also provides improved viewing
of cavitation.

Figure 12 shows the installation of a stationary hydrofoil in
the test section for the purpose of determining the effects of
Reynolds number on cavitation noise. Using this test setup a series
of four geometrically similar, but differently sized, hydrofoils
were tested. The variation of the noise associated with leading edge
sheet cavitation with Reynolds number was determined when the cavi-
tation cavity was 1/3 of the hydrofoil chord length, Figure 15.
This figure demonstrates the effect of laminar boundary layer
separation on cavitation and its noise. In separate flow visuali-
zation tests, the 3.81 and 7.62 cm chord hydrofoils were shown to be
experiencing a long and a short laminar separation bubble,
respectively. On the other hand, the 15.24 and 30.48 cm hydrofoils
experienced a non-separated turbulent boundary layer. The complete
results of this study can be found in Reference [15].

The cavitation noise radiated by a propeller can also be
determined from these test setups. The propeller can either be
mounted in an inclined position to duplicate the wake from the
drive shaft and struts, Figure 16, or with a model hull attached
to a flat plate which spans the test section, Figure 17. In both
cases the influence of the free surface and Froude scaling is
ignored. Using either of these installations it is possible to
determine the variation of propeller cavitation noise as a function
of Reynolds number. With these data it is possible to develop
model-to-prototype cavitation noise scaling laws if full-scale
data are available.

5.2 Non-Cavitating Noise

In addition to cavitation noise, the GTWT can be used to study
non-cavitating propeller noise. This is accomplished with an array
of 69 parallel-wired hydrophones located in a hydrodynamic fairing
at the end of the tunnel diffuser in front of the first set of
turning vanes, Figure 18. This sensor permits the far-field radiated
noise to be measured at frequencies > 300 Hz. When used in con-
junction with other sensors located in the test section, dual-
channel signal processing can be used to identify sources of propeller
noise and paths of propogation.

The measurement of non-cavitating model propeller noise requires
the model motor and drive system to operate with a minimum level of

mechanical noise in order to assure a sufficient propeller signal-
to-noise ratio. This is accomplished with a specially designed
quiet motor/dynamometer. The background noise spectrum is measured
with the quieted model motor/dynamometer operating with a tunnel
velocity and a rotating bare hub. When a model propeller is
installed on the model and operated at the same tunnel velocity
and RPM, its measured noncavitating noise is above the background
noise by the amount shown in Figure 19.

To study the mechanisms by which propellers and turbomachines
generate radiated noise, an air-breathing anechoic chamber is
available for operation with the Axial Flow Research Fan (AFRF).
This chamber has internal dimensions of 2.7 x 3.2 m and is anechoic
at frequencies above 230 Hz. It is equipped with polyurethane foam
wedges and provides a flow of air to the AFRF through its top and
bottom edges. The chamber can also operate as a stand-alone anechoic
chamber by removal of the AFRF.

Employing this arrangement and instrumentation to measure the
dynamic forces and pressures on the AFRF blades (these are described
in a later section), one can determine the acoustic transfer function
by conducting simultaneous measurements of the radiated noise. It
is also possible to determine the effects of blade geometry on
radiated noise since the AFRF is designed to accommodate systematic
changes in blade number, blade pitch angle and blade lift coefficient.

In all of the arrangements described above, the recording and
analysis of the acoustic signals are accomplished by a number of
real-time signal processors. The processed data can be transmitted
to a high-speed digital computer. Here the data are corrected for
hydrophone sensitivity and system gains and plotted in a format
consistent with the type of signal analysis performed. A block
diagram of this data reduction system is shown in Figure 20.

6.0 DYNAMIC FORCE TESTS

A major concern in the field of hydrodynamics is the generation
of dynamic forces on the propeller and hull of a marine vehicle since
this can result in excessive structural vibration. The ability to
control this vibration requires the capability to measure the hydro-
dynamic forces which cause the vibration. At ARL/PSU dynamic pro-
peller forces are measured either as the dynamic shaft thrust or as
the dynamic lift and moment on a section of the propeller.

On the other hand the measurement of the low frequency, essen-
tially quasi-steady, dynamic forces on a vehicle which is made to move
in a prescribed motion, can be used to determine the closed-loop con-
trol and maneuvering characteristics of the vehicle. These dynamic

forces are measured using a Planar Motion Mechanism which is operated
in the GTWT. These dynamic forces are then used to determine the
hydrodynamic stability derivatives on models of completely submerged
vehicles.

6.1 Dynamic Propeller Forces

        The measurement of the total dynamic response of a propeller at
ARL/PSU is limited to the measurement of the dynamic shaft thrust
alone. While the dynamic thrust is only one component of the entire
dynamic response of the propeller, it is a major component in most
cases. Further, the combination of accurate dynamic shaft thrust
measurements and an analytical method to predict all of the components
of the propeller dynamic shaft response permits the remaining
components to be inferred.

        The propeller dynamic shaft thrust dynamometer used at ARL/PSU
is shown in Figure 21. The sensor is a peizoelectric crystal which
reacts to the dynamic thrust through a hardened steel hemispherical
ball on the propeller hub. The dynamometer is designed to be
compliant only in the thrust direction and is located within the
propeller drive shaft. While the compliancy will limit the response
of the dynamometer at higher frequencies, experience has shown that
it is possible to obtain a flat sensor response to frequencies in
the order of 700 Hz. This is usually sufficient to permit the
measurement of the first- and second-harmonics of the dynamic thrust.

        This dynamometer has been used to study the dynamic shaft thrust
generated on a propeller operated in spatially non-uniform inflows
and in various temporally varying, turbulent, inflows. Some
typical results from these studies are shown in Figure 22, where
the measured dynamic thrust on a free-stream propeller operated
in a homogeneous turbulent inflow is shown. These measured values
are compared with predictions from a method by Thompson [16]. This
method also predicts all of the components of the dynamic force and
moment on the propeller shaft due to operation in a spatially non-
uniform inflow.

        To determine the mechanisms which cause the dynamic shaft
response of a propeller, it is necessary to study the dynamic response
of the individual blades. To accomplish this, a strain gage dynamo-
meter has been developed which measures the dynamic lift and moment
on a section of a rotating blade, Figure 23.

        To date this concept has been used with a rotor operated in the
AFRF. A series of tests has been conducted in spatially non-uniform
inflows to determine the effects of blade pitch angle (β), solidity
or expanded area ratio, and reduced frequency on the dynamic lift
and moment [17]. Such data provide the opportunity to assess the
various analytical methods which are available to predict the dynamic

lift and moment on a rotating blade. These data also provide insight
into what blade geometries will minimize the level of the blade's
dynamic response to a known non-uniform inflow.

While this individual blade dynamometer is limited in its
frequency response to < 160 Hz, it is possible to test at reduced
frequencies, based on the chord length, of nearly 10. The
definition of reduced frequency used here is:

$$2\pi \text{ (chord length) } \cos(\beta)/\text{(distortion wavelength)}$$

These values of reduced frequency are experienced in practice and
are obtained by using large blade chord lengths, 15.24 cm, and
varying the wavelength of the distorted inflow between 7.9 and
118 cm.

6.2 Planar Motion Mechanism

The prediction of the trajectory and dynamic motion of a marine
vehicle requires a knowledge of how the forces on the vehicle change
with time and vehicle attitude. This knowledge can be obtained by
forcing a model of the vehicle into a known time-dependent motion
and measuring the resulting forces. This permits the vehicle's
stability derivatives to be determined and used in the equations
of motion.

An accepted means to obtain the stability derivatives is to
conduct tests with a Planar Motion Mechanism (PMM). The CTWT has
been equipped with a PMM which is fitted to a special tunnel hatch
cover and permits the evaluation of small (d < 20 cm) axisymmetric
models, Figure 24. This system can drive the model in a pure
heaving motion as shown in Figure 24, a pure pitching motion by
having the actuators in phase, or in a combined motion. The maximum
frequency of oscillation is 10 Hz.

The unique feature of the GTWT PMM is that it can be used to
determine the effects of cavitation the vehicle's response and both
quasi-steady and dynamic hydrodynamic forces can be studied.

7.0 FLOW FIELD MEASUREMENTS

It is well recognized that an extremely important part of hydro-
dynamic testing is the ability to measure the velocity and pressure
fields associated with a particular test setup. As a result, the
development of pressure probes, hot-film and hot-wire probes, and
more recently laser Doppler velocimeters is a common undertaking in
a hydrodynamic test laboratory. While flow field measurements have
been a routine capability at ARL/PSU for many years, there have
been some recent developments which extend these capabilities.
These include: (1) the use of nylon mono-filament mini-tufts for

surface flow visualization; (2) the development of miniature 5-hole
probes with a total diameter of 1.67 mm; and (3) the measurement of
the flow field relative to a rotating propeller. Each of these
recent developments is described below.

7.1 Mini-Tuft Flow Visualization

The visualization of surface flows and flow separation with
small wool-tufts is a common practice in wind tunnel testing. The
adaptation of this method to water tunnels is difficult, however,
because of the wetting of the tufts. In both air and water the size
of the tufts can produce an interference with the surface flow and
result in a false conclusion. Following a development in the aero-
space field, ARL/PSU has demonstrated the use of nylon mono-filament
mini-tufts with a diameter of 0.03 mm in water [18].

These mini-tufts are attached to the surface with an epoxy
cement at the positions where the surface flows are of interest.
They are typically 12 mm in length and, as such, are barely visible
to the naked eye. To overcome this limitation the mono-filament is
coated with a fluorescent dye which makes them appear to be many
times their actual size when viewed in an ultravoilet light.
This provides a very effective means to visualize flow separation
without the problem of the markers interfering with the flow field.

While the use of these mini-tufts has been satisfactorily
demonstrated in the ARL/PSU 0.305 m diameter water tunnel, they
are still not operational in the 1.22 m GTWT. This restriction is
due to the inability to transmit enough ultraviolet light through
the GTWT windows and nearly 0.6 m of water to satisfactorily
illuminated the mini-tufts. This can probably be overcome by using
a stronger light source and windows which absorb less of the ultra-
violet light.

7.2 Miniature 5-Hole Probes

Five-hole pressure probes are common in all hydrodynamic labora-
tories [19]. One of the restrictions of commercially available
5-hole probes is their size and the subsequent interference effect
which they have on the flow, particularly shear flows such as the
wake behind a fin. As a result, many laboratories attempt to manu-
facture their own 5-hole probes to provide smaller overall dimensions.
At ARL/PSU such a development has lead to the use of a 5-hole probe
whose maximum diameter d = 1.67 mm.

The usefulness of this probe is shown in Figure 25 where the
vector sum of the radial and tangential components of the velocity
downstream of a set of stationary fins is plotted. This representa-
tion clearly shows the tip vortices and detailed wake structure
associated with each fin. The ability of these small probes to

measure this kind of detail provides a more exact Fourier representation of the flow field, which is important in the analysis of the dynamic response of a propeller.

7.3 Flow Relative to a Rotating Propeller

The hydrodynamic propeller designer is always concerned with the flow field relative to the blades of a rotating propeller. In the past this information has been lacking since it is extremely difficult to obtain. However, the development of the laser doppler velocimeter provides a technique which makes these measurements possible.

The data acquisition system employed at ARL/PSU to measure the velocities relative to a rotating propeller is shown in Figure 26. The heart of this system is the data control system which was designed and built at ARL/PSU. This system receives a signal from an encoder attached to the rotating shaft, takes this signal and chooses the correct instant when the laser beam is to be focused at a pre-selected position relative to the rotating propeller, accepts the scattered light at that instant and passes on to the next point. By changing the specified position it is possible to obtain a survey of the velocity field relative to the propeller. Figure 27 is an example of such a survey.

The AFRF is a specialized airflow facility for the study of axial-flow turbomachinery rotor and stator. It also has the capability to conduct flow surveys relative to the rotating blades, but using conventional probes. The rotor hub is large enough to house a special mechanism which rotates with the rotor and will position a probe within the channel between the blades. This mechanism is described in Reference [20].

8.0 SUMMARY

This report has presented a brief discussion of the major improvements that have occurred in the test capabilities of the ARL/PSU hydrodynamic test facilities during the past ten years. These advances include the development of (1) corrections for tunnel wall interference on powered model drag measurements, (2) electro-optic techniques for measuring cavitation nuclei distributions and velocity fields, (3) techniques to study cavitation damage using high velocity flows, (4) the capability to measure cavitating and non-cavitating propeller noise, (5) dynamometers to measure propeller and model dynamic forces, and (6) improved methods to measure and visualize hydrodynamic flow fields.

9.0 REFERENCES

[1] Ross, D., J. M. Robertson and R. B. Power, "Hydrodynamic Design
     of the 48-inch Water Tunnel at the Pennsylvania State Univer-
     sity," SNAME TRANSACTIONS, Vol. 56, pp. 5-29, 1948.

[2] Lehman, A. F., "The Garfield Thomas Water Tunnel," Ordnance
     Research Laboratory Report NORD 16597-56, September 1959.

[3] Lehman, A. F. and T. E. Peirce, "The Garfield Thomas Water
     Tunnel," UNDERWATER MISSILE PROPULSION, Ed L. Greiner, Compass
     Publications, Inc., Arlington, VA, pp. 401-420, 1967.

[4] Lehman, A. F., J. H. Light and T. E. Peirce, "Elimination of
     Water-Tunnel Interaction With a Coaxial Test Body by a Flow-
     Correcting Liner," Ordnance Research Laboratory Report NORD
     16597-39, July 1958.

[5] Peirce, T. E., "Tunnel Wall Interference Effects on Drag and
     Pitching Moment of an Axisymmetric Body," Ph.D. Thesis,
     Pennsylvania State University, December 1964.

[6] Billet, M. L. and E. M. Gates, "A Comparison of Two Optical
     Techniques for Measuring Cavitation Nuclei," TRANSACTIONS OF
     ASME, JOURNAL OF FLUIDS ENGINEERING, Vol. 103, pp. 8-13, 1981.

[7] Ward, T. M., "The Hydrodynamics Laboratory at the California
     Institute of Technology," TRANSACTIONS OF ASME, JOURNAL OF
     FLUIDS ENGINEERING, Vol. 98, pp. 740-748, 1976.

[8] Gates, E. M., "The Influence of Free-Stream Turbulence, Free-
     Stream Nuclei Populations and Drag Reducing Polymers on Cavita-
     tion Inception," California Institute of Technology, Division
     of Engineering and Applied Science, Report No. 183-2, 1977.

[9] Keller, A. P., "The Influence of the Cavitation Nucleus on Cavi-
     tation Inception, Investigated With the Light Scattering Method,"
     TRANSACTIONS OF ASME, JOURNAL OF BASIC ENGINEERING, Vol. 94,
     pp. 917-925, 1972.

[10] Billet, M. L. and C. B. Yungkurth, "Light Scattering System:
Analysis and Calibration," ASME Symposium on Measurements in
Polyphase Flows, St. Louis, MO, June 1982.

[11] Arakeri, V. H. and A. J. Acosta, "Cavitation Inception Obser-
vations on Axisymmetric Bodies at Supercritical Reynolds
Numbers," JOURNAL FOR SHIP RESEARCH, Vol. 20, No. 1, pp.
40-50, 1976.

[12] Gates, E. M., M. L. Billet, J. Katz, K. K. Ooi, J. W. Holl,
A. J. Acosta, "Cavitation and Nuclei Distributions - Joint
ARL/CIT Experiments," California Institute of Technology,
Division of Engineering and Applied Science, Report No. E 244.1,
September 1979.

[13] Stinebring, D. R., J. W. Holl and R. E. A. Arndt, "Two Aspects
of Cavitation Damage in the Incubation Zone: Scaling by
Energy Considerations and Leading Edge Damage," TRANSACTIONS
OF ASME, JOURNAL OF FLUIDS ENGINEERING, Vol. 102, pp. 481-485,
1980.

[14] Lauchle, G. C., "Acoustic Characteristics of the ARL/FEU
Ellipsoidal Reflecting Hydrophone," Applied Research Laboratory
TM 76-15, February 1976.

[15] Billet, M. L. and D. E. Thompson, "Blade Surface Cavitation
Noise," PROCEEDINGS OF ASCE, IAHR/AIHR and ASME JOINT
SYMPOSIUM ON FLUID MACHINERY, Vol. II, Fort Collins, CO,
June 1978.

[16] Thompson, D. E., "Propeller Time-Dependent Forces Due to Non
Uniform Inflow," Ph.D. Thesis, Pennsylvania State University,
1976.

[17] Bruce, E. P., "Axial Flow Rotor Unsteady Performance," Ph.D.
Thesis, Pennsylvania State University, 1979.

[18] Stinebring, D. R. and A. L. Treaster, "The Use of Fluorescent
Mini-Tufts for Hydrodynamic Flow Field Visualization," Applied
Research Laboratory TM 80-07, January 1980.

[19] Treaster, A. L. and A. M. Yocum, "The Calibration and Application
of Five-Hole Probes," Instrument Society of America Transactions,
Vol. 18, No. 3, pp. 23-34, 1979.

[20] Pierzga, M. J., "Experimental Verification of the Streamline
Curvature Numerical Analysis Method Applied to the Flow
Through an Axial Flow Fan," M.S. Thesis, Pennsylvania State
University, 1980.
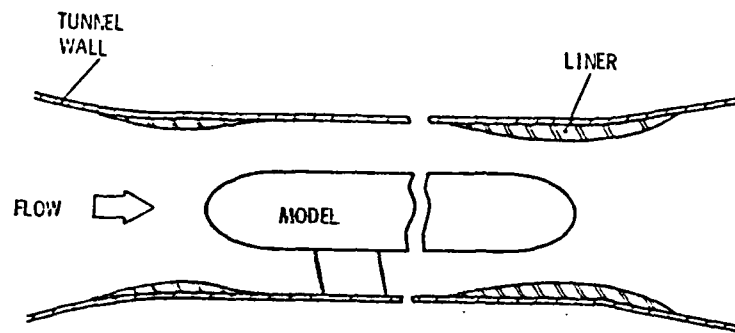
Figure 1. Installation of Model With Tunnel Wall Liner in GTWT
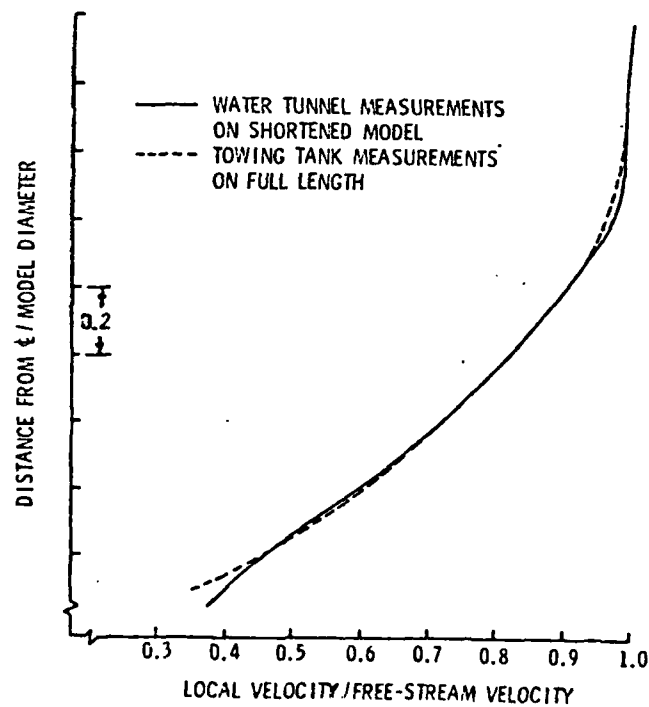
Figure 2. Comparison of 0.61 m Diameter Model Velocity Profile
Measured in Water Tunnel and Towing Tank
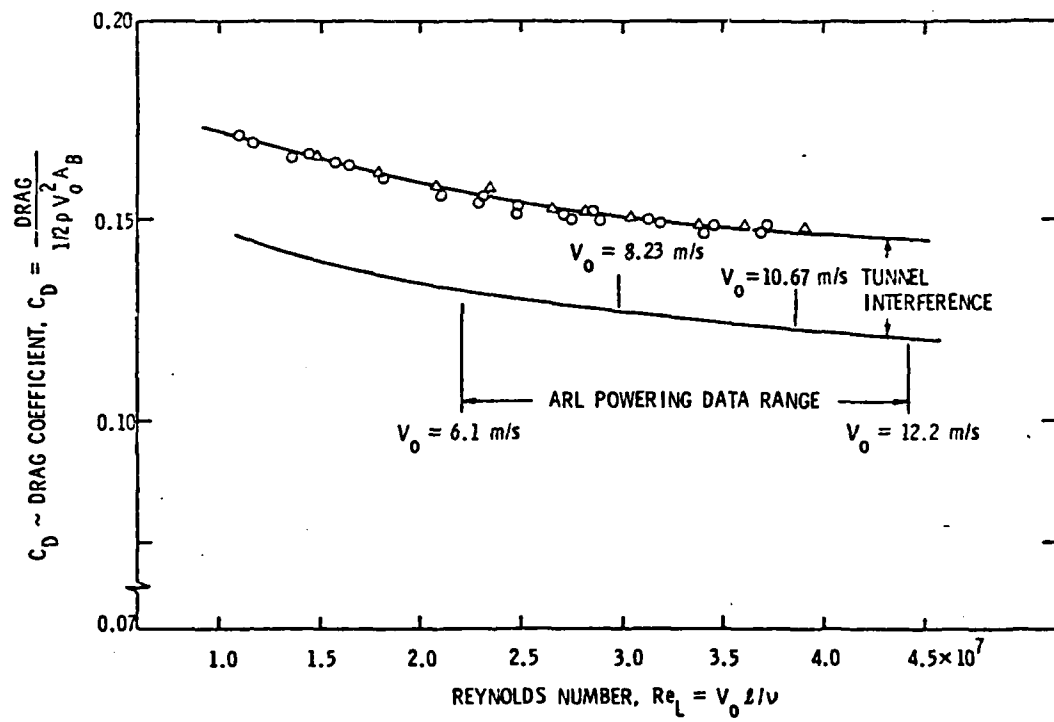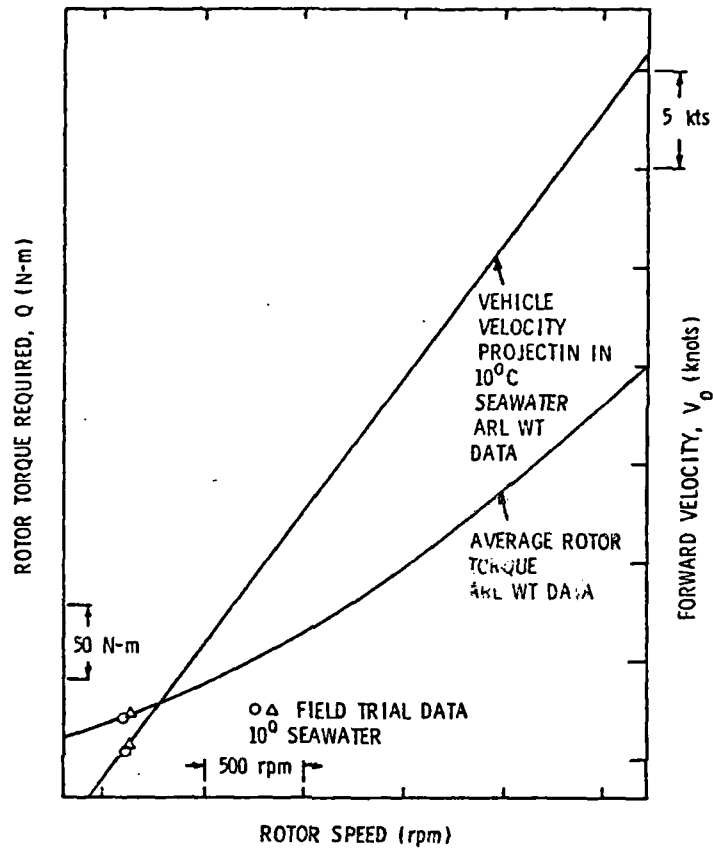
Figure 3. C_D vs Reynolds; Determination of Wall Interference
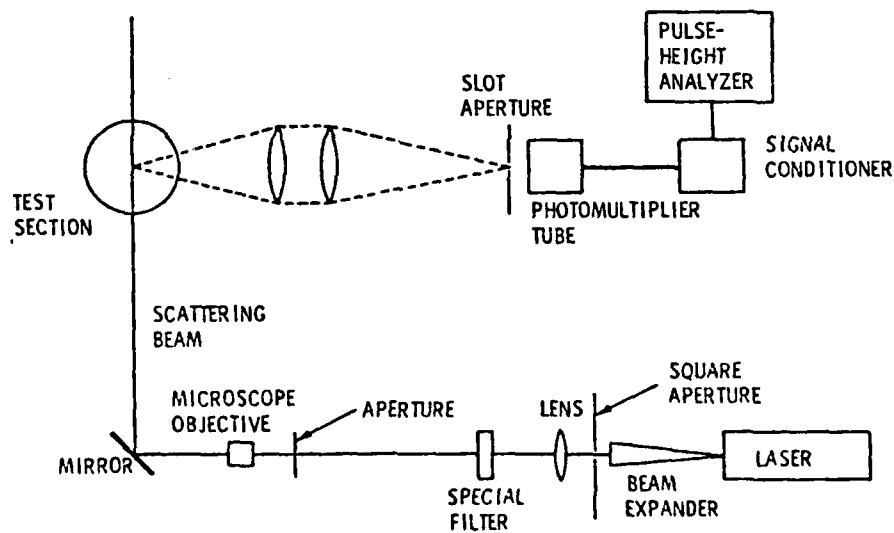
Figure 4. Comparison of Water Tunnel and Free-Field Propulsion Data

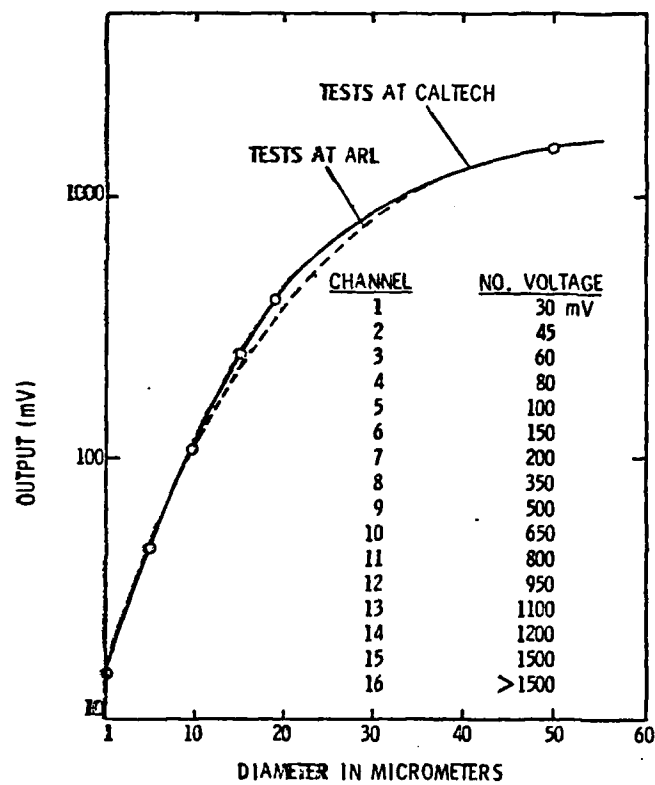Figure 5. Schematic of the Light Scattering Nuclei Counter

Figure 6. Calibration of Light Scattering Nuclei Counter at
CIT and ARL/PSU
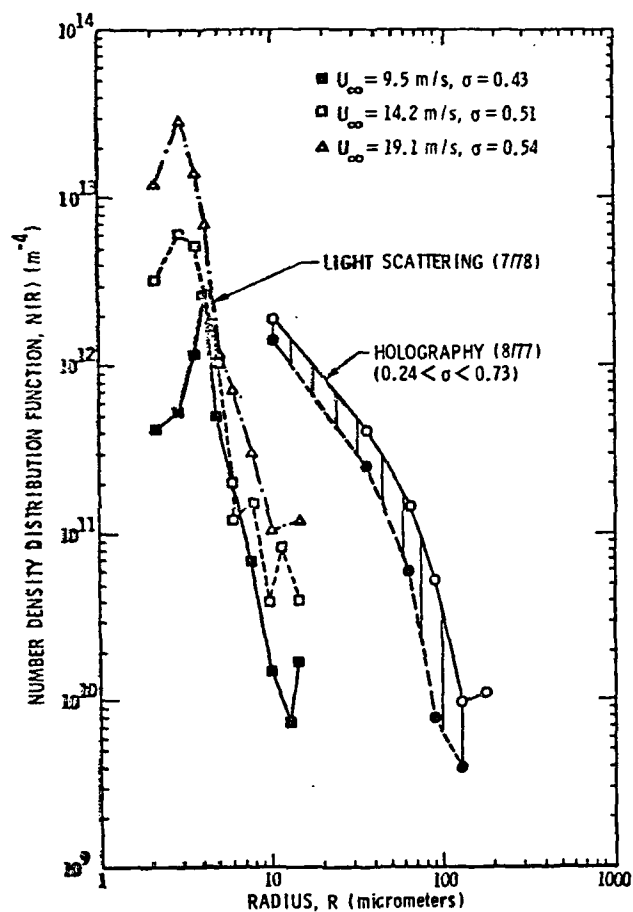
Figure 7. A Comparison of Nuclei Distributions Measured in Light Scattering and Holographic Systems
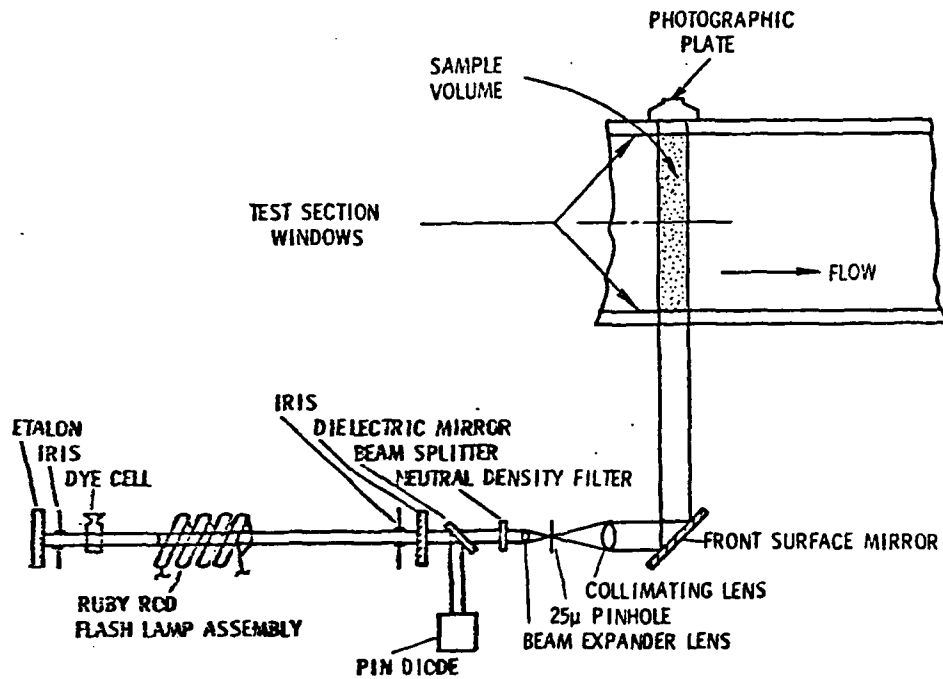
Figure 8. Schematic of Holographic System
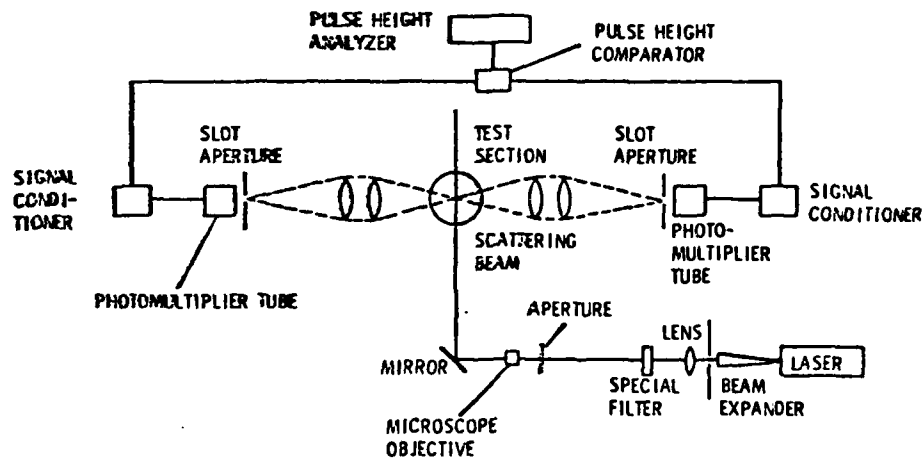
Figure 9. Schematic of the Dual-Detector Light Scattering System
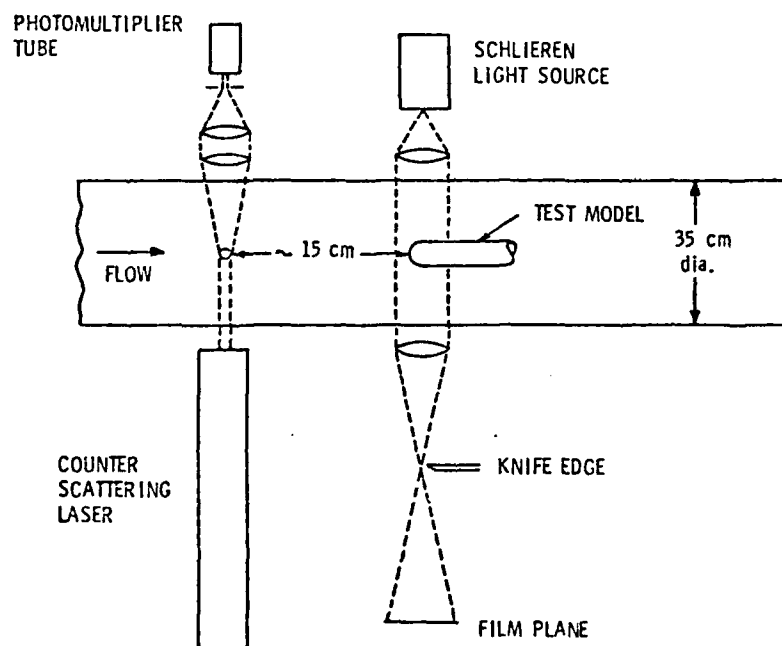
Figure 10.   Schematic of the Schlieren Flow Visualization and Laser
Light Scattering Systems
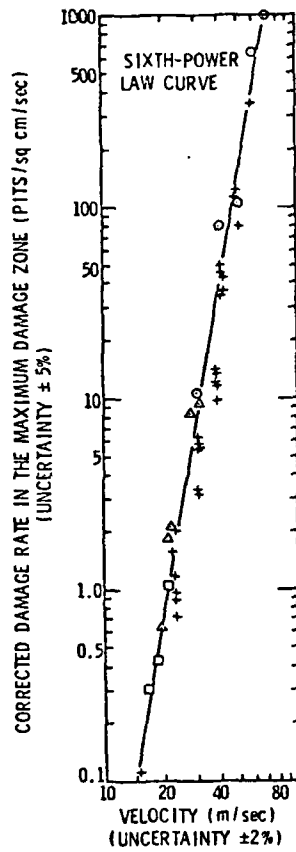
Figure 11.   Damage Rate Versus Velocity From Various Investigations
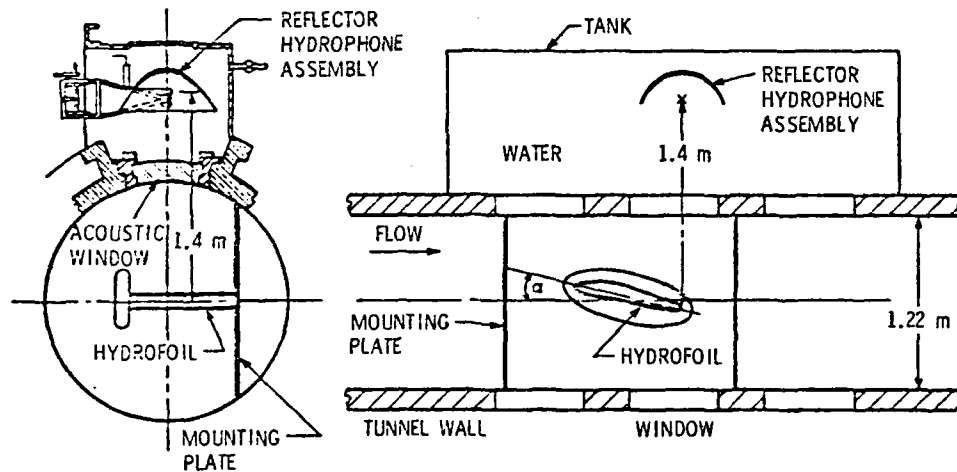
Figure 12. Acoustic Tank and Reflector Hydrophone Arrangement
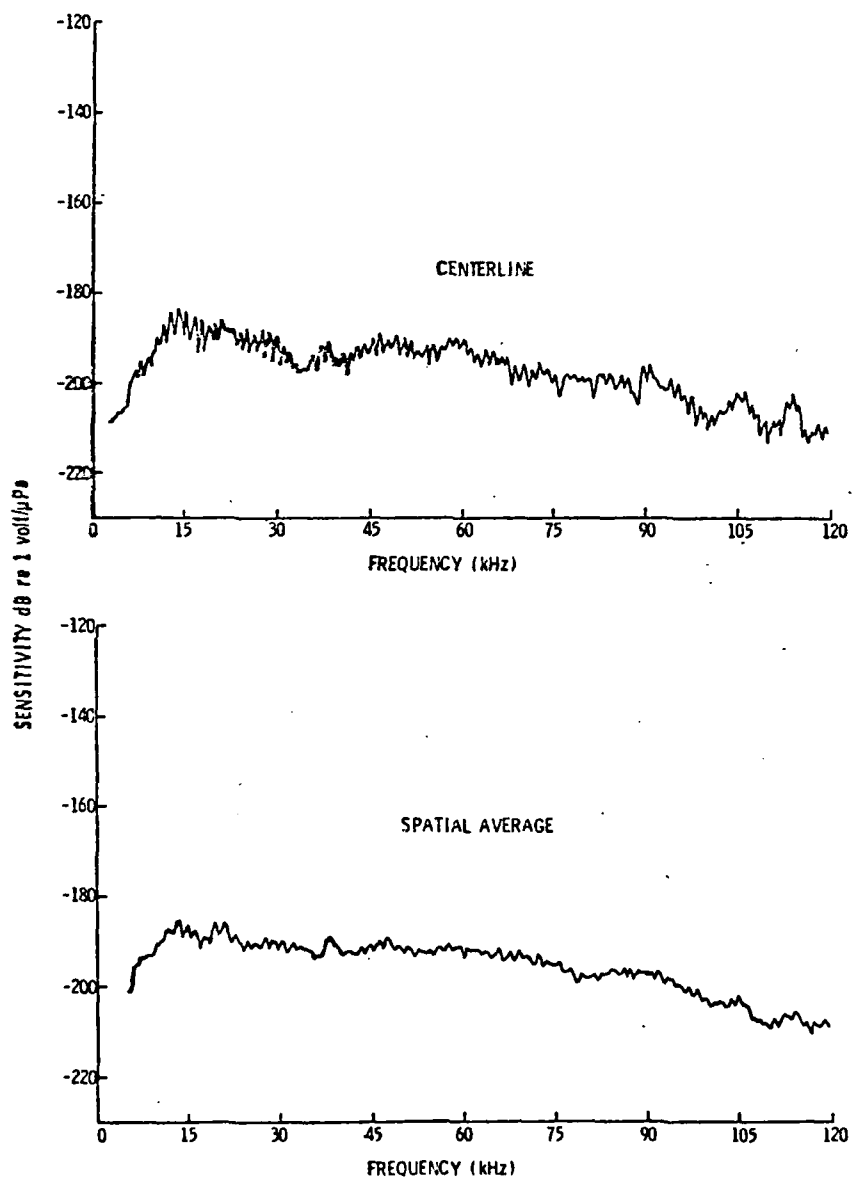
Figure 13. Typical Sensitivity Curves for Reflector Hydrophone
(5-120 kHz) With Projector on Centerline and Spatially-
Averaged for Several Projector Locations off Centerline
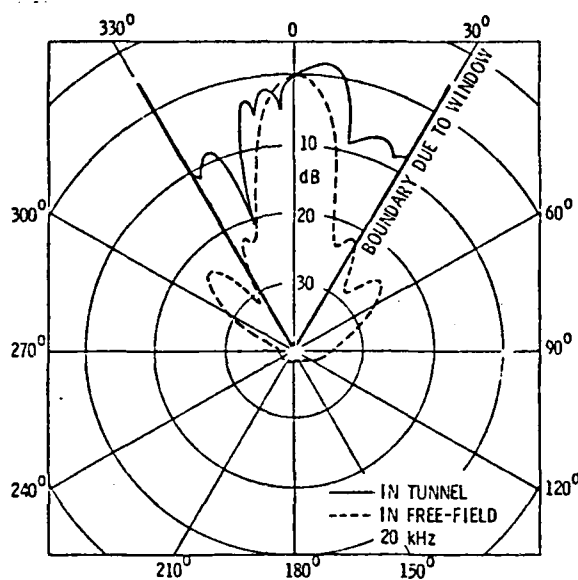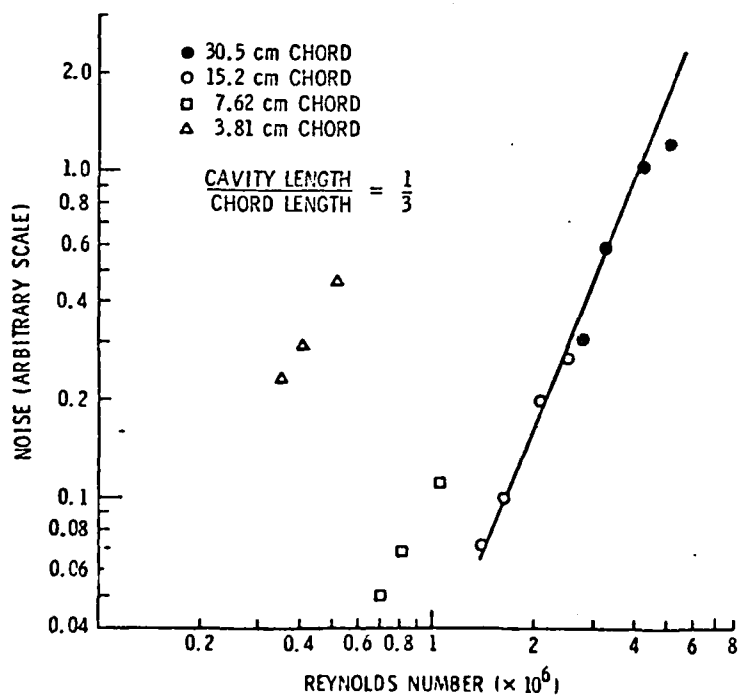
Figure 14.   Reflector Hydrophone Directivity @ 20 kHz

Figure 15.   RMS Noise Level of Leading Edge Sheet Cavitation Versus
Reynolds Number

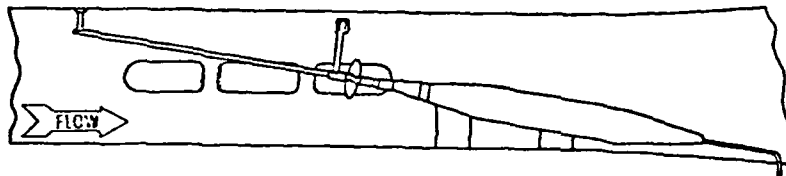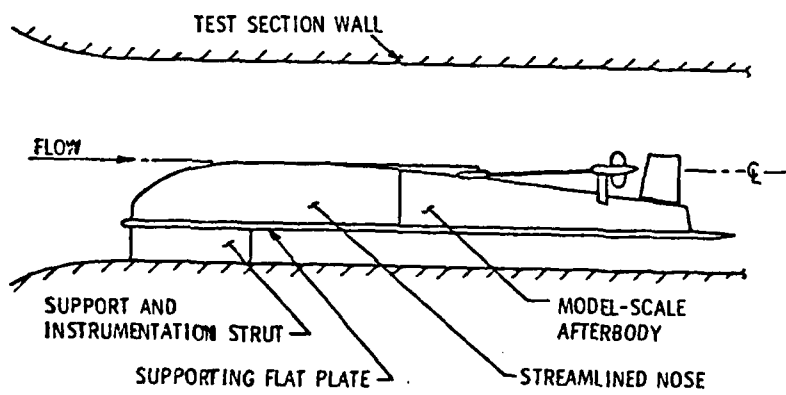**Figure 16.** Installation of Ship Propeller in an Inclined Flow in GTWT

Figure 17. Installation of a Ship Model Hull and Propeller in GTWT

Figure 18. GTWT Downstream Array
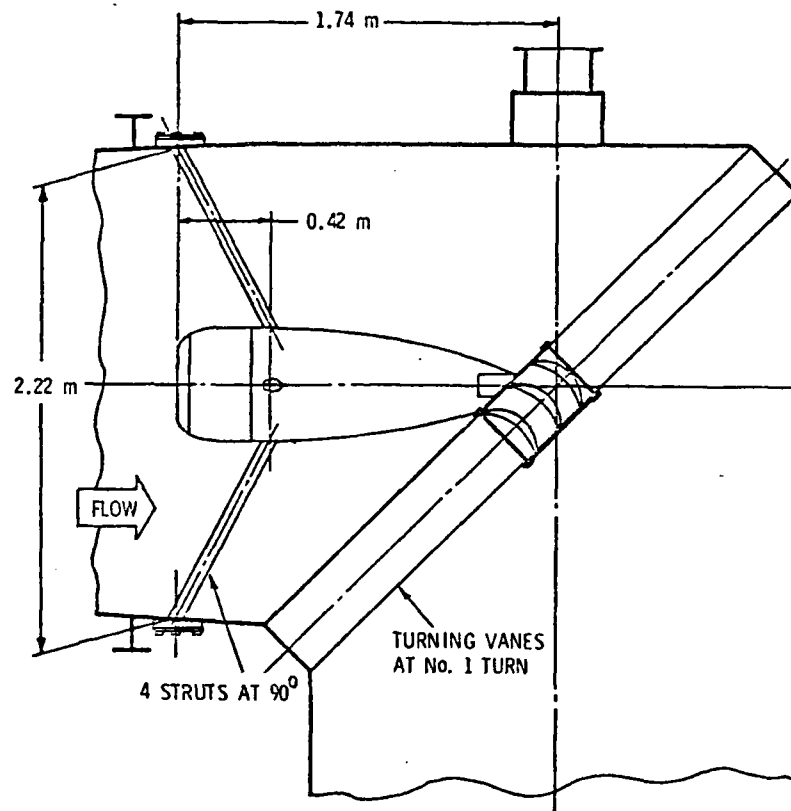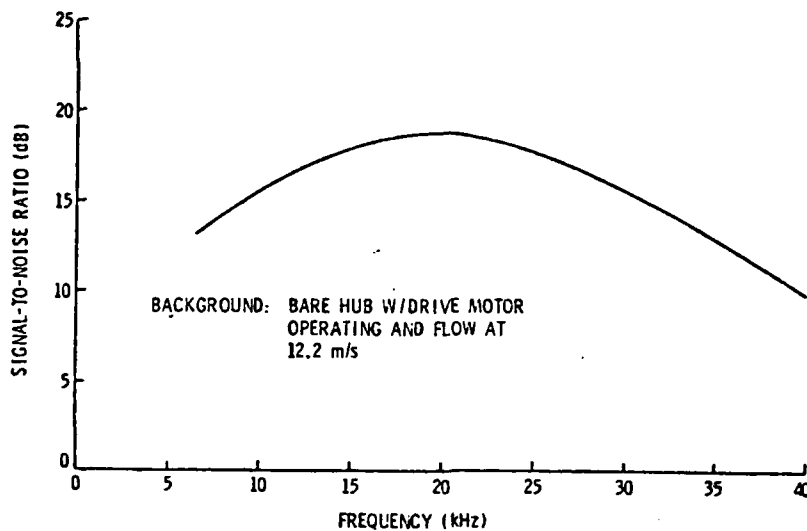
Figure 19. Typical Signal-to-Noise Ratio Measured With Non-Cavitating
Propeller in GTWT
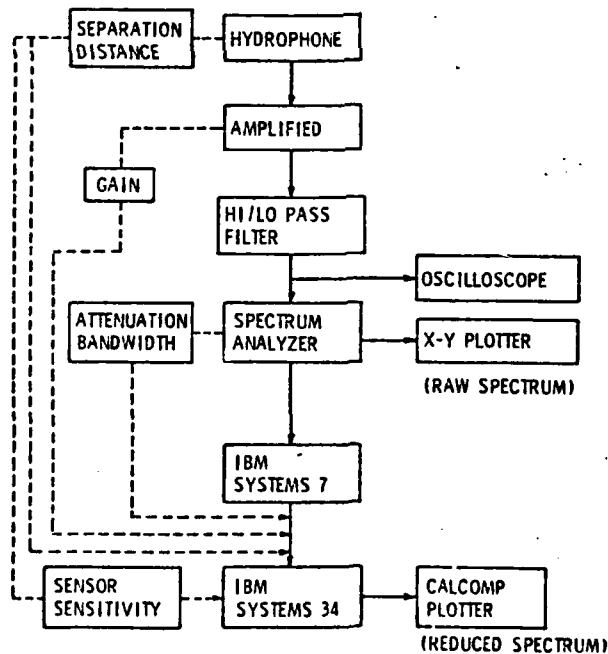

Figure 20. Block Diagram of Noise Data Reduction System

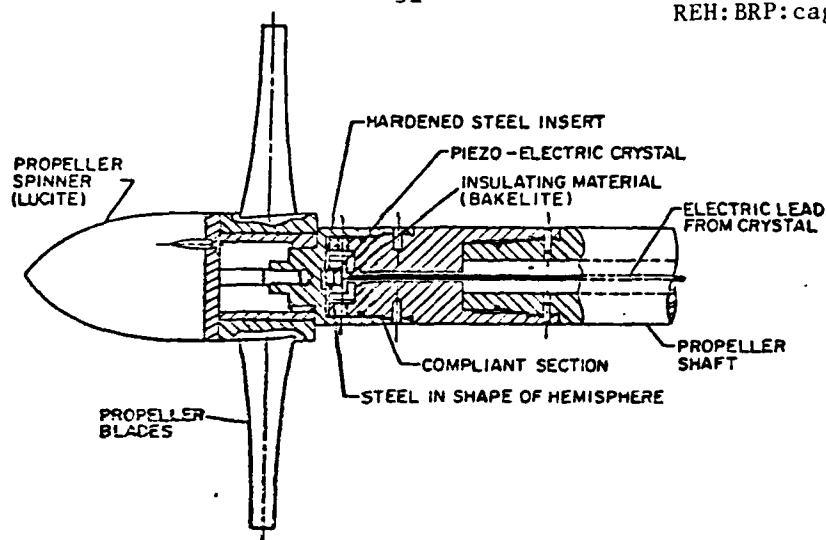Figure 21. Dynamic Shaft Thrust Dynamometer
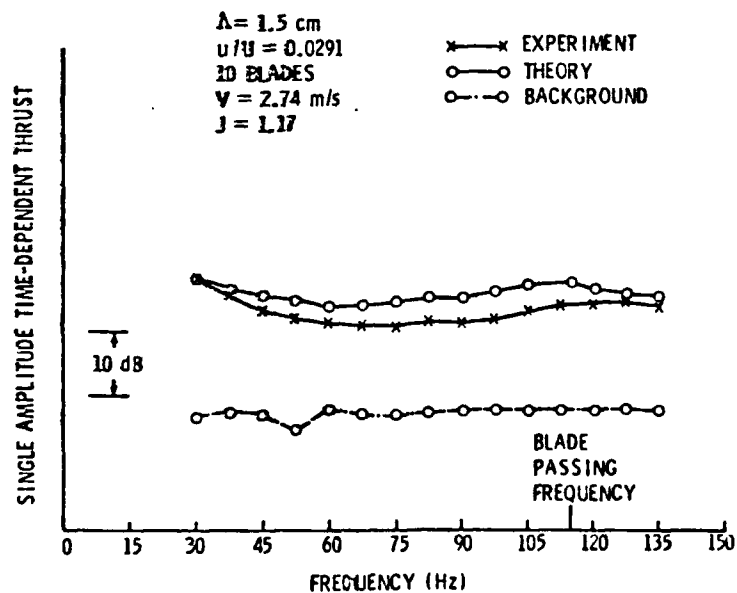
Figure 22. Turbulence Generated Dynamic Shaft Thrust
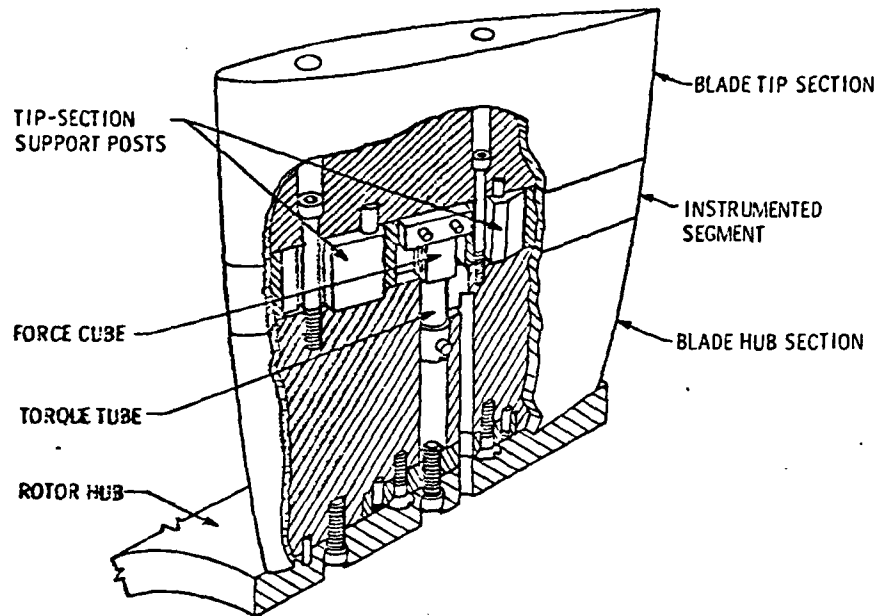
Figure 23. Dynamic Lift and Moment Dynamometer for a Rotating Blade

Figure 24. CTWT Planar Motion Mechanism

Figure 25.   Radial and Tangential Velocity Vectors Measured Behind
a Set of Stationary Fins

Figure 26.   Laser Doppler Velocimeter for Measuring Velocities
Relative to a Rotating Propeller

Figure 27.   Axial Velocity Behind a Rotating Propeller; Relative
to the Propeller

APPENDIX: FACILITY OPERATING CHARACTERISTICS

APPLIED RESEARCH LABORATORY, FLUIDS ENGINEERING DEPARTMENT   (USA)
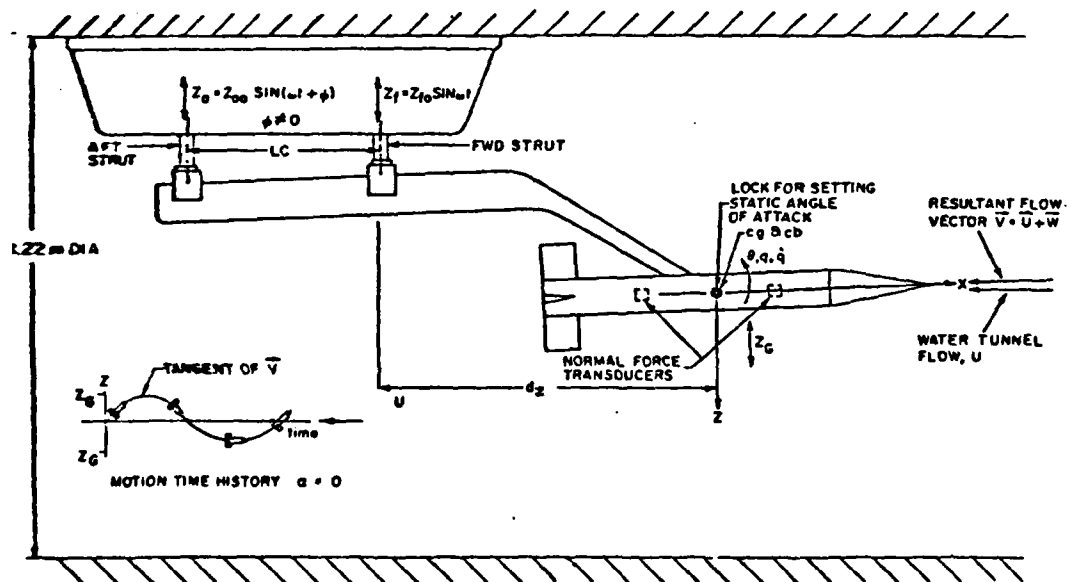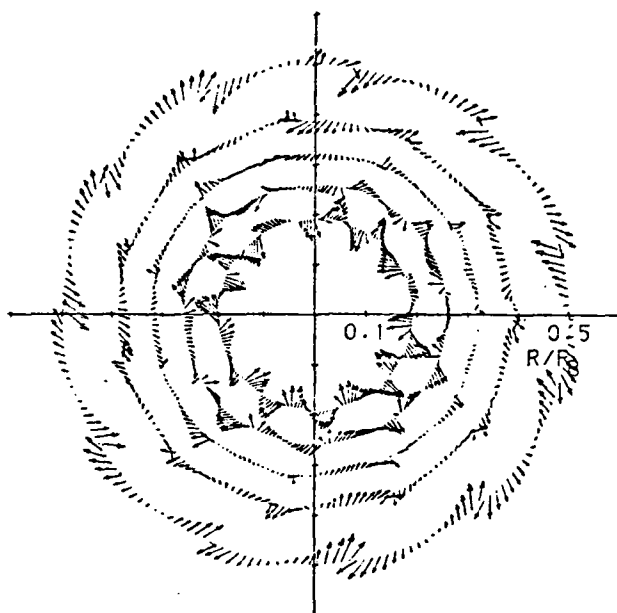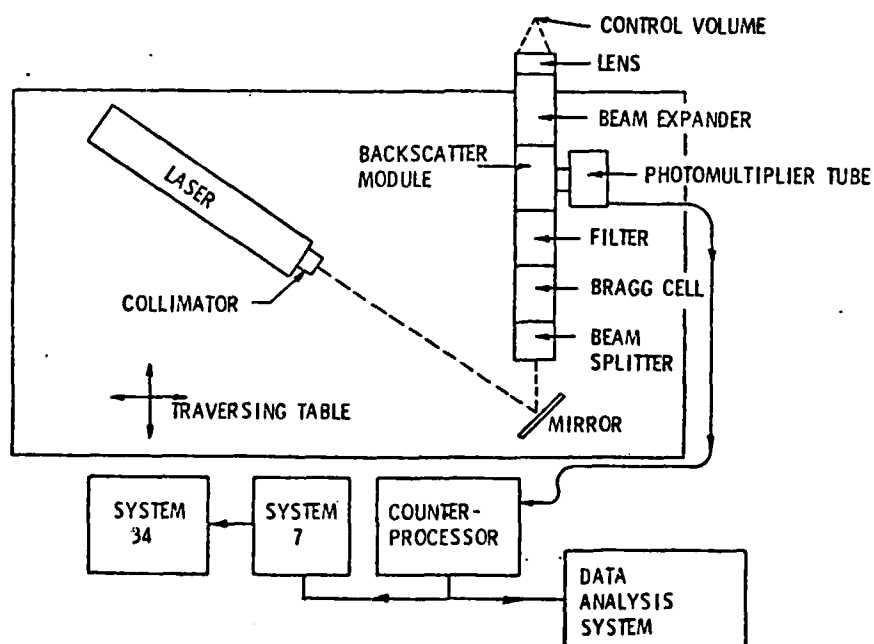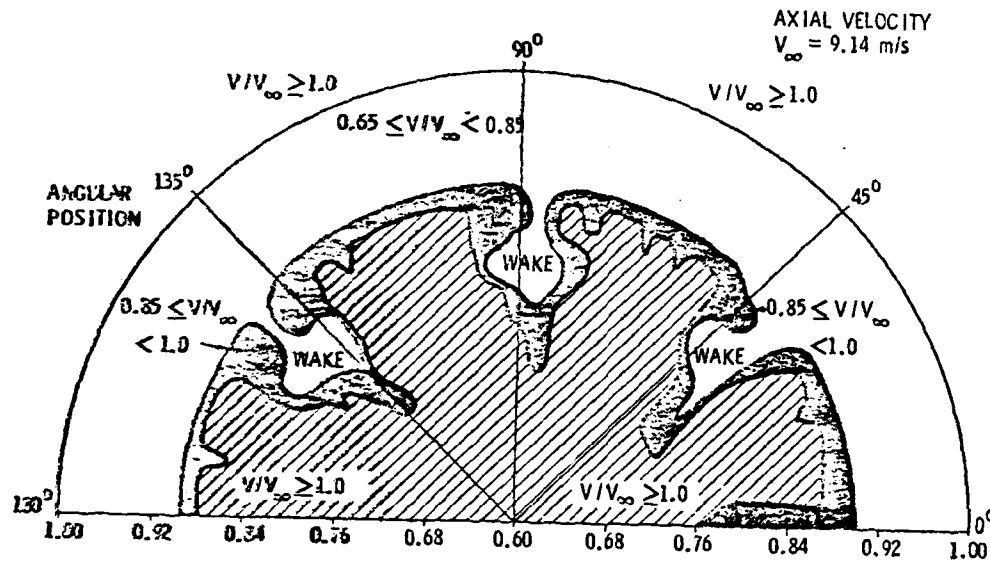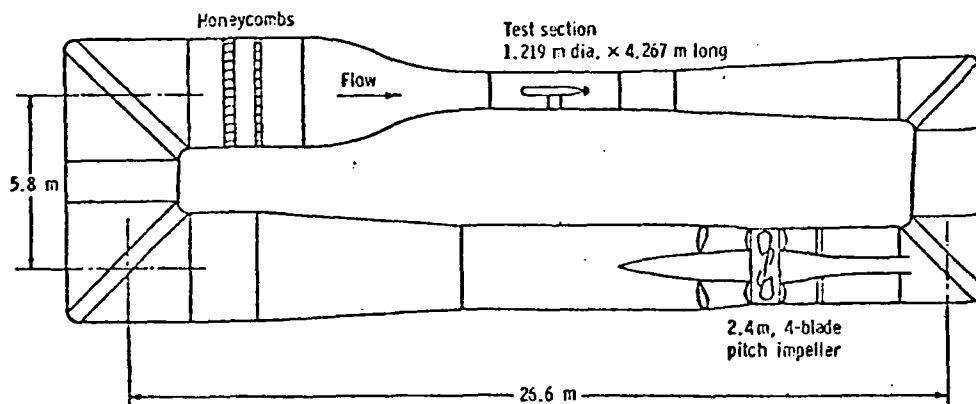THE PENNSYLVANIA STATE UNIVERSITY
P. O. BOX 30, STATE COLLEGE, PA 16801   (814) 865-1741
CAVITATION TUNNEL (Garfield Thomas)   1949

DESCRIPTION OF FACILITY: Closed Circuit, Closed Jet

TYPE OF DRIVE SYSTEM: 4-Blade Adjustable Pitch Impeller

TOTAL MOTOR POWER: 2000 HP Variable Speed (1491 kw)

WORKING SECTION MAX. VELOCITY: 18.29 m/s

MAX. & MIN. ABS. PRESSURES: 413.7 to 20.7 kPa

CAVITATION NUMBER RANGE: >0.1 dependent on velocity and/or J-range

INSTRUMENTATION: Propeller Dynamometers, 5-Hole Pitot Probes, Lasers, Pressure
Sensors, Hydrophones, Planar Motion Mechanism, Force Balances

TYPE AND LOCATION OF TORQUE & THRUST DYNAMOMETERS: Model internally mounted,
140 HP limit. (104.40 kw)

PROPELLER OR MODEL SIZE RANGE: Model size from 76.2 mm to 635.0 mm dia.

TESTS PERFORMED: (1) Forces and pressure distributions on bodies of revolution,
hydrofoils, propellers, etc., (2) Cavitation performance and noise measurements
of propellers, foils, hydrodynamic shapes, etc., (3) Steady state and time-
dependent force and torque measurements on powered models.

OTHER REMARKS: Tunnel turbulence level is 0.1 percent in test section. Air
content can be controlled as low as 1 ppm per mole. Measurement can be made
of hydrodynamic functions for stability and control of submerged vehicles.
Directional hydrophone system for relative acoustic measurements.

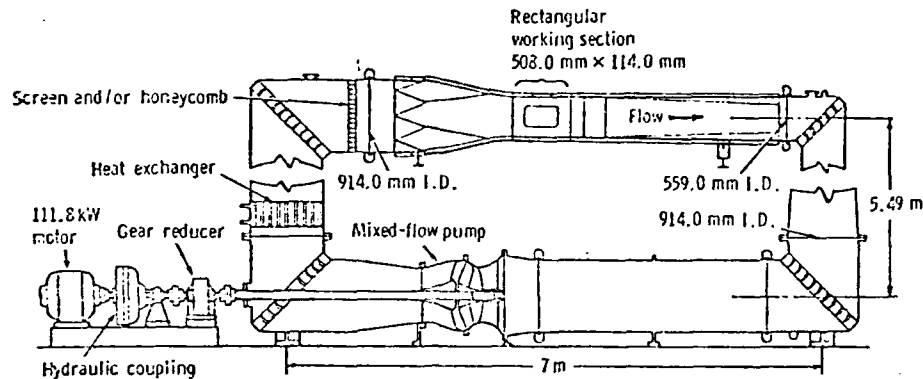PUBLISHED DESCRIPTION: ARL/PSU Report NORD 16597-56, Lehman, 1959

APPLIED RESEARCH LABORATORY, FLUIDS ENGINEERING DEPARTMENT   (USA)
THE PENNSYLVANIA STATE UNIVERSITY
P. O. BOX 30, STATE COLLEGE, PA 16801   (814) 865-1741
CAVITATION TUNNEL   1951

DESCRIPTION OF FACILITY: Closed Circuit, Closed Jet

TEST SECTIONS: 1) Circular: 304.8 mm dia. x 762.0 mm long
                                  2) Rectangular: 508.0 mm x 114.3 mm x 762.0 mm
                                      long

TYPE OF DRIVE SYSTEM: Mixed Flow Peerless Pump

TOTAL MOTOR POWER: 150 HP (111.8 kw)

WORKING SECTION MAX. VELOCITY: 24.38 m/s

MAX. & MIN. ABS. PRESSURES: 413.7 to 20.7 kPa

CAVITATION NUMBER RANGE: >0.1 dependent on velocity

INSTRUMENTATION: Lasers, pressure sensors, hydrophones

MODEL SIZE RANGE: 50.8 mm max. dia.

TESTS PERFORMED: Steady and time dependent force and pressure measurements
on unpowered models. Noise measurements on cavitating models. Three-
dimensional flow problems—circular section. Two-dimensional flow problems—
rectangular section. Axial-flow pump tests.

OTHER REMARKS: Independent gas control of air content. Water filtration with
25-micrometer filters. Intermittent operation with drag-reducing additive
injection. Partial neutralization of additive downstream of test section.

PUBLISHED DESCRIPTION: ARL/PSU Report NORD 16597-56, Lehman, 1959

APPLIED RESEARCH LABORATORY, FLUIDS ENGINEERING DEPARTMENT   (USA)
THE PENNSYLVANIA STATE UNIVERSITY
P. O. BOX 30, STATE COLLEGE, PA 16801   (814) 865-1741
CAVITATION TUNNEL   1962
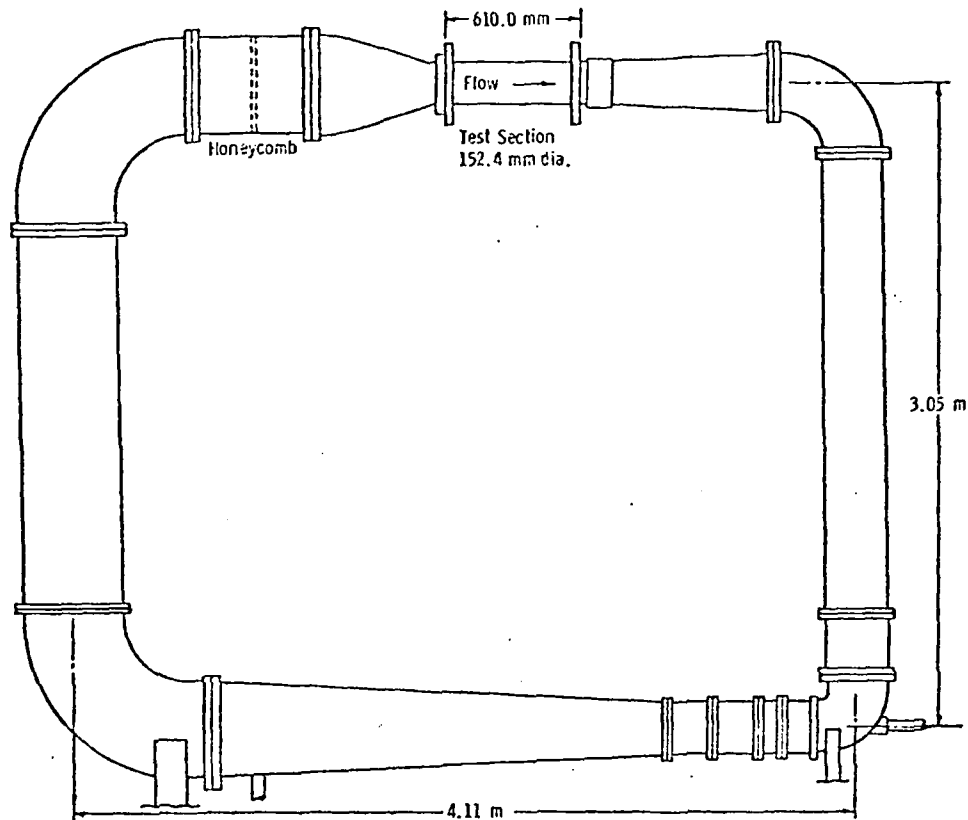
DESCRIPTION OF FACILITY: Closed Circuit, Closed Jet

TYPE OF DRIVE SYSTEM: Axial-Flow Pump

TOTAL MOTOR POWER: 25 HP   (18.64 kw)

WORKING SECTION MAX. VELOCITY: 21.34 m/s

MAX. & MIN. ABS. PRESSURES: 861.9 to 20.7 kPa

CAVITATION NUMBER RANGE: >0.1 dependent on velocity and pressure

INSTRUMENTATION: Pressure Transducers

TEMPERATURE: Ambient

TESTS PERFORMED: Effect of polymers on axial-flow pumps. Surface roughness
effects on cavitation.

OTHER REMARKS: Air content control by vacuum pump. Filtration of solid
particles and non-Newtonian additives by activated charcoal.

PUBLISHED DESCRIPTION: PSU M.S. Thesis, Kaku, 1962

APPLIED RESEARCH LABORATORY, FLUIDS ENGINEERING DEPARTMENT   (USA)
THE PENNSYLVANIA STATE UNIVERSITY
P. O. BOX 30, STATE COLLEGE, PA 16801   (814) 865-1741
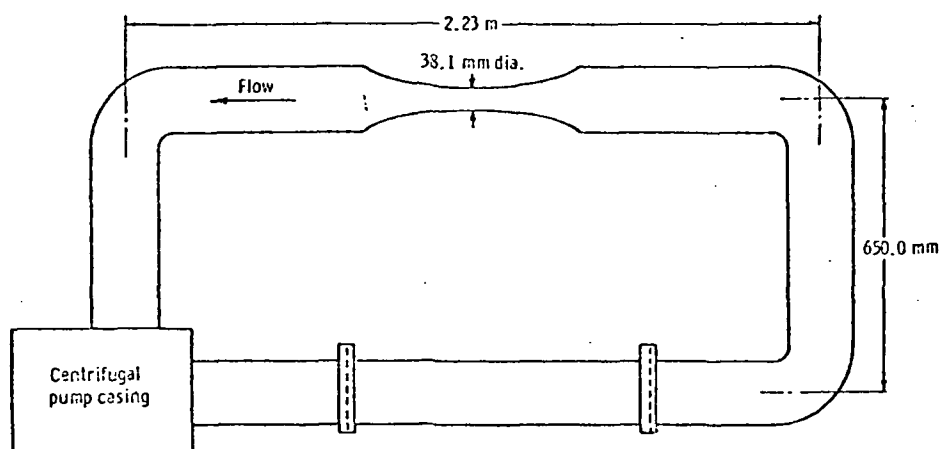ULTRA-HIGH SPEED CAVITATION TUNNEL   1960

DESCRIPTION OF FACILITY:	Closed Circuit, Closed Jet
TYPE OF DRIVE SYSTEM:	Centrifugal Variable Speed Drive
TOTAL MOTOR POWER:	75 HP (55.9 kw)
WORKING SECTION MAX. VELOCITY:	83.8 m/s
MAX. & MIN. ABS. PRESSURES:	8274.0 to 41.4 kPa
CAVITATION NUMBER RANGE:	>0.01 dependent on pressure and velocity

INSTRUMENTATION: Pressure and temperature sensors

TEMPERATURE RANGE: 16°C to +176°C

MODEL SIZE RANGE: 12.7 mm max. dia.

TEST MEDIUM: Water, Freon 113, Alcohol

TESTS PERFORMED: Incipient and desinent cavitation studies. Developed
cavitation studies. Cavitation damage.

OTHER REMARKS: Stainless steel tunnel. Bronze pump. Three filter banks for
removal of water, acids, solid particles (10 micrometers).

PUBLISHED DESCRIPTION: ARL/PSU TM 75-188, Weir, Billet & Holl, 1975

APPLIED RESEARCH LABORATORY, FLUIDS ENGINEERING DEPARTMENT   (USA)
THE PENNSLYVANIA STATE UNIVERSITY
P. O. BOX 30, STATE COLLEGE, PA 16801   (814) 865-1741
AXIAL FLOW RESEARCH FAN   :   1971

1. Bellmouth inlet
2. Disturbance-producing section
3. Disturbance-producing honeycomb
4. Support fins
5. Test section automated for
   flow-field surveys
6. Rotor test blades *
7. Stator test blades
8. Diffuser and test blade drive system
9. Auxiliary fan
10. Throttle
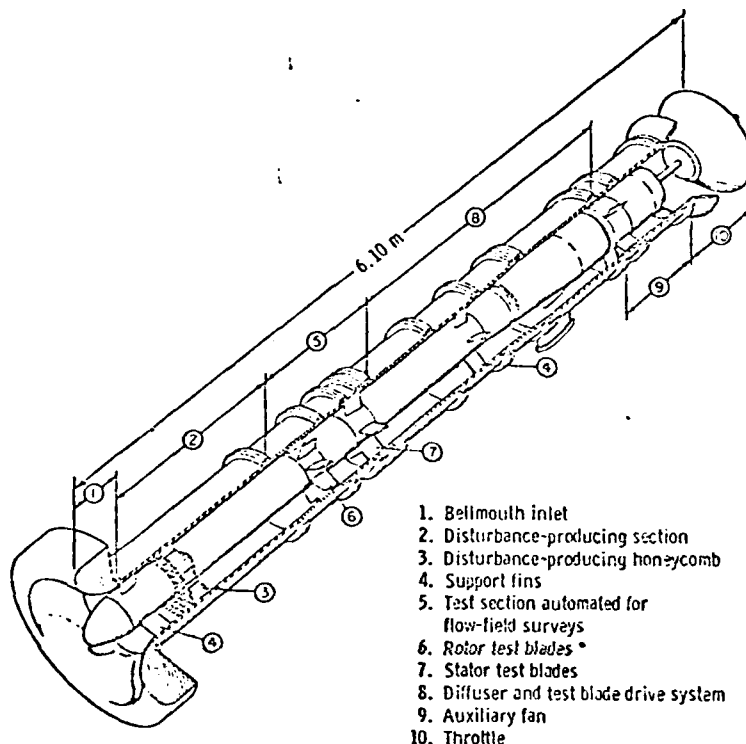
*540.0 mm O.D., 241.0 mm hub dia., 150.0 mm blade chord

DESCRIPTION OF FACILITY:	Open Circuit
TYPE OF DRIVE SYSTEM:	Single Axial Flow Stage
TOTAL MOTOR POWER:	20 HP (14.9 kw)
WORKING SECTION MAX. VELOCITY:	34.14 m/s through-flow velocity
MAX. RELATIVE VELOCITY:	91.44 m/s

INSTRUMENTATION: Variable geometry test stage. Instrumented blade for measuring unsteady lift and pitching moment. Rotating outer casing for flow surveys. Distortion screens to produce reduced frequencies between 0.25 and 5.0.

TESTS PERFORMED: Measurements in a distorted inflow of the unsteady lift, moment, surface pressures, instantaneous total pressure and time mean velocities and pressures, as a function of stage geometry and reduced frequency.

OTHER REMARKS: Facility was specifically built for research in the generating mechanism of turbomachinery noise and vibration, a problem which is of significance in many areas of engineering, including that of environmental pollution.

PUBLISHED DESCRIPTION: ARL/PSU TM 72-109, Bruce, 1972

Commander
Naval Sea Systems Command
Department of the Navy
Washington, DC 20362
Attn: Library
     Code NSEA-09G32
(Copy Nos. 1 and 2)

Naval Sea Systems Command
Attn: R. Keane
     Code NSEA-3213
(Copy No. 3)

Naval Sea Systems Command
Attn: C. Mussen
     Code PMS-3962
(Copy No. 4)

Naval Sea Systems Command
Attn: F. E. Eissing
     Code NSEA-05H
(Copy No. 5)

Naval Sea Systems Command
Attn: S. M. Blazek
     Code NSEA-05HB
(Copy No. 6)

Naval Sea Systems Command
Attn: A. R. Paladino
     Code NSEA-05H1
(Copy No. 7)

Naval Sea Systems Command
Attn: F. B. Peterson
     Code NSEA-052P
(Copy No. 8)

Naval Sea Systems Command
Attn: F. J. Welling
     Code NSEA-521
(Copy No. 9)

Naval Sea Systems Command
Attn: R. Taddeo
     Code NSEA-5212
(Copy No. 10)

Naval Sea Systems Command
Attn: E. G Liszka
     Code NSEA-63R1
(Copy No. 11)

Naval Sea Systems Command
Attn: F. J. Romano
     Code NSEA-63R3
(Copy No. 12)

Naval Sea Systems Command
Attn: T. E. Peirce
     Code NSEA-63R31
(Copy No. 13)

Naval Sea Systems Command
Attn: R. Cauley
     Code NSEA-052B
(Copy No. 14)

Naval Sea Systems Command
Attn: R. A. Johnson
     Code NSEA-03D35
(Copy No. 15)

Naval Sea Systems Command
Attn: C. D. Smith
     Code NSEA-06R
(Copy No. 16)

Naval Sea Systems Command
Attn: E. M. Peebles
     Code NSEA-92
(Copy No. 17)

Naval Sea Systems Command
Attn: D. M. Jackson
     Code NSEA-06B
(Copy No. 18)

Naval Sea Systems Command
Attn: T. M. Hopkins
     Code NSEA-05
(Copy No. 19)

Naval Sea Systems Command
Attn: M. V. Ricketts
     Code NSEA-03
(Copy No. 20)

Commanding Officer
Naval Underwater Systems Center
Newport, RI 02840
Attn: D. Goodrich
     Code 3634
(Copy No. 21)

DISTRIBUTION LIST FOR UNCLASSIFIED ARL TM No. 82-66 by R. E. Henderson and
B. R. Parkin, dated 12 February 1982.

Naval Underwater Systems Center
Attn: B. J. Myers
        Code 36311
(Copy No. 22)

Naval Underwater Systems Center
Attn: R. H. Nadolink
        Code 3634
(Copy No. 23)

Naval Underwater Systems Center
Attn: R. Kittredge
        Code 36301
(Copy No. 24)

Naval Underwater Systems Center
Attn: Library
        Code 54
(Copy No. 25)

Officer-in-Charge
David W. Taylor Naval Ship R&D Center
Department of the Navy
Annapolis Laboratory
Annapolis, MD   21402
Attn: E. R. Quandt
        Code 272
(Copy No. 26)

David W. Taylor Naval Ship R&D Center
Attn: J. V. Pierpoint
        Code 2741
(Copy No. 27)

David W. Taylor Naval Ship R&D Center
Attn: J. Henry
        Code 2741
(Copy No. 28)

David W. Taylor Naval Ship R&D Center
Attn: Y. F. Wang
        Code 2740
(Copy No. 29)

Commander
David W. Taylor Naval Ship R&D Center
Department of the Navy
Bethesda, MD   20084
Attn: W. B. Morgan
        Code 15
(Copy No. 30)

David W. Taylor Naval Ship R&D Center
Attn: Library
        Code 1505
(Copy No. 31)

David W. Taylor Naval Ship R&D Center
Attn: W. G. Day
        Code 1521
(Copy No. 32)

David W. Taylor Naval Ship R&D Center
Attn: A. C. Lin
        Code 1521
(Copy No. 33)

David W. Taylor Naval Ship R&D Center
Attn: R. A. Cumming
        Code 1540
(Copy No. 34)

David W. Taylor Naval Ship R&D Center
Attn: J. H. McCarthy
        Code 154
(Copy No. 35)

David W. Taylor Naval Ship R&D Center
Attn: T. E. Brockett
        Code 1544
(Copy No. 36)

David W. Taylor Naval Ship R&D Center
Attn: M. M. Sevik
        Code 19
(Copy No. 37)

David W. Taylor Naval Ship R&D Center
Attn: W. K. Blake
        Code 1905
(Copy No. 38)

David W. Taylor Naval Ship R&D Center
Attn: F. S. Archibald
        Code 1942
(Copy No. 39)

Commander
Naval Surface Weapons Center
Silver Spring, MD   20910
Attn: Library
(Copy No. 40)

DISTRIBUTION LIST FOR UNCLASSIFIED ARL TM No. 82-66 by R. E. Henderson and
B. R. Parkin, dated 12 February 1982.

Office of Naval Research
Department of the Navy
800 N. Quincy Street
Arlington, CA 22217
Attn: A. H. Gilmore
(Copy No. 41)

Office of Naval Research
Attn: Adm. Kollmorgen
(Copy No. 42)

Office of Naval Research
Attn: R. Whitehead
(Copy No. 43)

Office of Naval Research
Attn: C. Lee
(Copy No. 44)

Commanding Officer
Naval Ocean Systems Center
San Diego, CA 92152
Attn: Library
(Copy No. 45)

Naval Ocean Systems Center
Attn: M. M. Reischmann
(Copy No. 46)

Naval Ocean Systems Center
Attn: D. Nelson
(Copy No. 47)

Naval Ocean Systems Center
Attn: J. Green
(Copy No. 48)

Defense Technical Information Center
5010 Duke Street
Cameron Station
Alexandria, VA 22314
(Copy Nos. 49 to 54)

Commanding Officer
Naval Underwater Systems Center
Newport, RI 02840
Attn: P. Tabor
(Copy No. 55)

Naval Underwater Systems Center
Attn: P. LaBrecque
(Copy No. 56)

Dr. G. F. Wislicenus
351 Golf Court (Oakmont)
Santa Rosa, CA 95405
(Copy No. 57)

J. M. Robertson
125 Talbot Laboratory
University of Illinois
Urbana, IL 61801
(Copy No. 58)

The Pennsylvania State University
Applied Research Laboratory
Post Office Box 30
State College, PA 16801
Attn: M. L. Billet
(Copy No. 59)

Applied Research Laboratory
Attn: W. S. Gearhart
(Copy No. 60)

Applied Research Laboratory
Attn: G. B. Gurney
(Copy No. 61)

Applied Research Laboratory
Attn: W. R. Hall
(Copy No. 62)

Applied Research Laboratory
Attn: J. W. Holl
(Copy No. 63)

Applied Research Laboratory
Attn: G. C. Lauchle
(Copy No. 64)

Applied Research Laboratory
Attn: F. E. Smith
(Copy No. 65)

Applied Research Laboratory
Attn: D. E. Thompson
(Copy No. 66)

Applied Research Laboratory
Attn: A. L. Treaster
(Copy No. 67)

Applied Research Laboratory
Attn: R. E. Henderson
(Copy No. 68)

DISTRIBUTION LIST FOR UNCLASSIFIED ARL TM No. 82-66 by R. E. Henderson and
B. R. Parkin, dated 12 February 1982.

Applied Research Laboratory
Attn: B. R. Parkin
(Copy No. 69)

Applied Research Laboratory
Attn: GTWT Files
(Copy No. 70)

R. Leitner
DARPA (TTO)
1400 Wilson Blvd.
Arlington, VA 22209
(Copy No. 71)

DATE
ILMED

8

SUPPLEMENTARY

INFORMATION

THE PENNSYLVANIA STATE UNIVERSITY
INTERCOLLEGE RESEARCH PROGRAMS AND FACILITIES
APPLIED RESEARCH LABORATORY

ADDRESS REPLY TO:

APPLIED RESEARCH LABORATORY
P. O. Box 30
STATE COLLEGE, PENNSYLVANIA 16801

August 10, 1982

TO: Distribution List

SUBJECT: Corrected Page for ARL Technical Memorandum

    A typographical error has been found on the first line of Page 8 of ARL TM 82-66, "Hydrodynamic Test Facilities at ARL/PSU," by R. E. Henderson and B. R. Parkin, 12 February 1982.

    Please replace Page 7-8 in your copy(ies) with the attached.

Very truly yours,

Blaine R. Parkin
Director
Garfield Thomas Water Tunnel

BRP:mac

was concluded from these experiments that the light scattering tech-
nique was not able to discriminate between solid particles and air
bubbles in the flow.

As a result of these findings, recent studies at ARL/PSU have
concentrated on the development of a dual-detector technique which,
with the use of Mie-scattering theory, can give information about the
shape of the particle. This permits the light scattering technique
to discriminate between microbubbles and particulates, Figure 9.
The results to date indicate that this modified Keller system offers
the potential of screening particulates from the microbubble counts
[10]. The main task remaining before this approach can be called
successful is to conduct a detail error analysis in order to resolve
the system inaccuracy introduced by the data reduction algorithm.
Because the light scattering technique offers the chance of getting
nearly real-time nuclei distribution data while a cavitation test
is in progress, this improvement of the Keller system is worth
pursuing.

Assuming that valid nuclei size distributions can be obtained
while a cavitation experiment is underway, the question of how such
distributions influence the development of cavitation on a body must
be studied. Such a study can be conducted if the cavitation events
can be related to such flow features as the boundary layer thickness
or whether or not the flow is separated. Schlieren flow visualization
is an effective way to show the relationship of cavitation inception
and its type to the state of the boundary layer [11]. Measurements of
this type have been performed in the ARL/PSU 0.305 m tunnel using
light scattering and schlieren systems simultaneously as illustrated
in Figure 10 [12].

Of course holographic photography can be used for flow visualiza-
tion with excellent results in both cavitating and non-cavitating
flows.

4.2 Cavitation Damage

In the introductory remarks of this section it was noted that
one use of the NASA tunnel and its very high velocity, has been to
study the process of cavitation damage [13]. Recent studies at
ARL/PSU have confirmed the sixth-power of the free-stream velocity
scaling relation reported by previous investigators. In these
studies it was possible to obtain nearly a four-fold increase in
velocity, from about 15 m/s to 60 m/s. A fact not previously
reported is that the pitting rate in the incubation zone is sensitive
to, and inversely proportional to, the dissolved air content.
Therefore it was possible to correct all of the data to a standard
air content of 8.9 ppm so that data for all investigations over a
10,000 to 1 range in damage rates could be brought into remarkable
agreement, Figure 11. It is important to stress that this investi-

gation involved the study of pitting on a body without the occurrence of weight loss. With this restriction it was found that damage in the form of individual pits had a one-to-one correspondence with the cavitation bubble collapse energy, and the change in this energy with free-stream velocity could be inferred.

5.0 ACOUSTIC TESTS

The GTWT was designed to provide the capability to conduct research on torpedo propellers operated in a specified vehicle/ control fin wake [1]. With the wake flow produced by the installation of the actual vehicle or a scaled model, the measurement of the forces on the vehicle and its propeller and the occurrence of cavitation on the propeller were the primary performance characteristics studied. While the inception of cavitation was detected acoustically, as well as visually, the GTWT was not used to conduct detailed acoustic tests during its first 20 years of operation. Fortunately, the design of the GTWT was directed towards quiet and vibration free operation. The success in achieving these goals has permitted the development of a capability to conduct tests of both cavitating and non-cavitating propeller noise.

5.1 Cavitation Noise

The GTWT was designed so that one side of its test section could be fitted with an acoustic tank in which a traversing reflector hydrophone could be mounted, Figure 12. With the hydrophone focused on the centerline of the test section, it measures the noise radiated from a model located opposite the 27 cm x 60 cm plexiglass windows.

The receiver is a Celesco LC-10 hydrophone located at the focus of the ellipsoidal reflector. This hydrophone is calibrated by placing an omni-directional sound projector with a known response in the test section and driving it over a frequency range of 1-120 kHz. The calibration is conducted with the sound projector located on the test section centerline and at a constant distance off-centerline in each of four or more circumferential positions, Figure 13. This latter approach permits an average sensitivity to be determined diminishes the influence of spurious acoustic modes that are observed when the projector is on the centerline. It is also more representative of the noise radiated by a propeller since cavitation will normally appear first near the tip of the blades.

The influence of the test section on the directivity of the reflector hydrophone is shown by Figure 14. In this figure the directivity measured at 20 kHz in the test section is compared with the same measurement conducted in the free field [14]. It is obvious that this arrangement is acceptable if the hydrophone is positioned in the center of the window, but is restricted by the metal webs between the windows. To overcome this restriction an